

Evaluation of Earthquake Demands for Concentrically Braced Steel Frame Buildings



C.-H. Chen

National Chiao Tung University

S. A. Mahin

University of California, Berkeley

SUMMARY:

This study examined the seismic demands of 3-, 6- and 16-story tall special concentrically braced frame (SCBF) archetype buildings for performance-based earthquake engineering (PBEE). The archetypes were subjected to SAC ground motion suite corresponding to hazard levels of 50%, 10% and 2% probabilities of exceedence in 50 years (the service-, design- and MCE-level events, respectively) for downtown Los Angeles to assess the likely demands at various hazard levels. Analyses show that low-rise archetypes exhibit higher probability of collapse at the MCE-level event. In the case study of two-story SCBF archetypes, reducing the response modification factor (R-factor) from 6.0 to 3.0 efficiently reduces the drift demands for low-rise SCBFs at various hazard levels. Therefore, the period-dependent R-factor is suggested for the design of SCBFs in the United States. Other engineering demand parameters discussed in this study includes drift ratios, peak floor accelerations, out-of-plane deformation of braces, and ductility demands of braces.

Keywords: SCBF; engineering demand; response modification factor; probability of collapse

1. INTRODUCTION

Conventional special concentrically braced frames (SCBF) have been widely used due to their efficiency in resisting lateral forces. Under severe lateral loading, braces will buckle, laterally and locally, leading to a deterioration of the strength and stiffness of the SCBF and under repeated excursions of cyclic inelastic deformation to fracture of braces. The collapse resistance of SCBF system was examined at the hazard level of 2% probabilities of exceedence in 50 years according to FEMA P695 methodology (FEMA 2009; Chen and Mahin 2010). The low-rise braced frame archetype buildings have higher probabilities of collapse at the hazard level of 2% probabilities of exceedence in 50 years than taller ones. The simulation results for the three-story tall, code-conforming braced frame buildings show that the probability of fracturing at least in one brace at the MCE-level event is over 70 percent in SCBF buildings. Fracture of braces significantly reduced the lateral strength and stiffness of the buildings and increased the probability of the collapse of these buildings (Uriz and Mahin 2008).

To investigate how the braced structural systems perform under earthquakes, a few of the archetypes are selected in this study. The 3-, 6- and 16-story tall archetypes are chosen to represent SCBF system having short to long periods.

2. STRUCTURAL SYSTEM INFORMATION

The archetype design carefully follows ASCE/SEI 7-05 design requirements. The beam-column connections and brace-to-framing connections of the archetypes are not designed in detail. It is assumed that these connections have adequate stiffness and strength, and are detailed so they will not fail before the braces rupture.

2.1. Design of Model Buildings

Three archetypes were designed for SCBFs representing 3-, 6-, and 16-story buildings, namely 3SCBFDmaxSAC, 6SCBFDmaxSAC and 16SCBFDmaxSAC. Fig. 2.1 shows the typical layout of the archetypes. The braced bays were located at the perimeter of the structures. For the 3 and 6-story archetypes, one bay of braced frame was used in each side of the perimeter. For the 16-story archetypes, two nonadjacent bays of braced frame were used in each side of the perimeter. The story height for all archetypes was 15 ft. The floor plan was 180 ft by 120 ft. Beam spans were 30 ft typically.

The importance factor and redundancy factor were assumed to be unity for all designs. Table 2.1 lists some of the principal attributes of the structures and the key parameters used in the seismic design. The archetypes intend to cover braced frames in the short and long period range. The archetypes are designed considering a soil site (Site Class D) condition and the resulting design lateral loads are based on $S_s = 1.5g$ and $S_1 = 0.6g$.

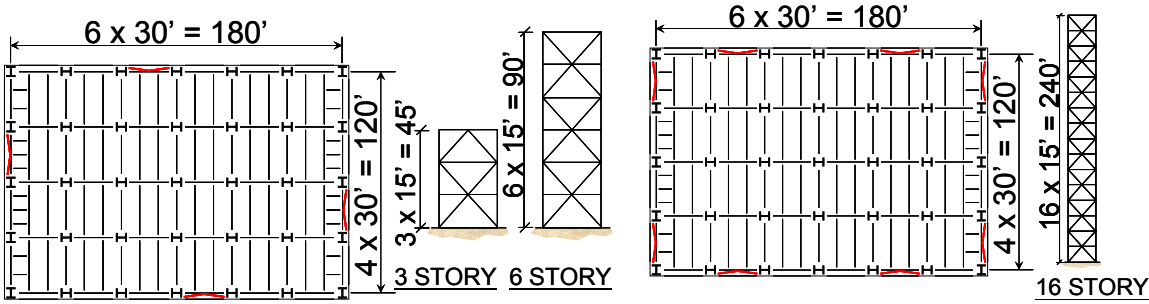


Figure 2.1. Typical layout of SCBF archetypes

Table 2.1. Design parameters of model buildings

Model	SCBFDmax
Code	ASCE/SEI 7-05
Soil Site	Site Class D
Seismic Design Category	D
Occupancy Category	II (Office)
Importance Factor	1.0
Short Period Spectral Acceleration, S_s	1.5g
1 sec. Period Spectral Acceleration, S_1	0.6g
F_a	1.0
F_v	1.5
R, Ω, C_d	6, 2, 5
Design Base Shear	0.167W (3-Story), 0.162W (6-Story), 0.059W (16-Story)

All of the braces in the archetype buildings are assumed to have pin connections to the framing. This is for the sake of simplicity for these analyses. Rigid in plane offsets are assumed at the beam-column connections and brace-to-framing connections. The effective length of the braces corresponds to 70% of the work-point-to-work-point length.

The gravity load only framing system is simplified as being a leaning column in the design. The P-delta effects are considered by applying gravity load on the leaning columns. The gravity columns are assumed to be axially rigid, but to have no lateral resisting capacity.

The braced frames are idealized as 2-D frames, and are designed assuming that all structural members are adequately braced laterally to avoid adverse torsional behavior. Any rotation of the floor diaphragms about a vertical axis is also ignored. As such, torsional effects due to mass and stiffness eccentricities, or premature deterioration of bracing on one side of the building, are not accounted for in the design or response analyses.

The structure was analyzed considering sixty ground motion records. These records were taken from the SAC ground motion ensembles developed consistent with 1997 NEHRP seismic hazard curves for

Los Angeles (Somerville 1997). The sixty records represent three different hazard levels (2% probability of exceedence in 50 years (the MCE-level events), 10% in 50 years (the design-level events) and 50% in 50 years (the service-level events)).

2.2. OpenSees Numerical Models

The archetype structures are simulated using two-dimensional plane frame models with a leaning column, as shown in Fig. 2.2. The analytical models of the archetypes are implemented in OpenSees (McKenna 1997). The columns are assumed continuous and are fixed to the base for all the nonlinear models. The beams are rigidly connected to the columns. At connections with gusset plates, the behavior is very nearly fixed, even if such connections are not detailed as being fully restrained. The braces including the gusset plates in the ends were modeled with force-based nonlinear beam-column element. Fiber sections were used for the critical sections where yielding might occur. The beam and columns were modeled similarly to capture inelastic behavior. A corotational formulation was used to model member buckling while local buckling was not explicitly modeled. An empirical cycle counting method was used to simulate rupture due to low-cycle fatigue (Uriz and Mahin 2008). The vertical floor mass tributary to the braces intersecting a beam or column was included in the models. Earlier studies (Khatib and Mahin 1988) showed that this vertical mass has a significant effect on dynamic response during brace buckling. $P-\Delta$ effects were represented using a leaning column. The leaning column was constrained to have the same lateral displacement as the most adjacent column at a level in the braced bay. The axial and flexural stiffness of the columns are assumed to be large, but a pin was introduced at the bottom of the column in each story. Fatigue material properties are included in the lateral resisting frame.

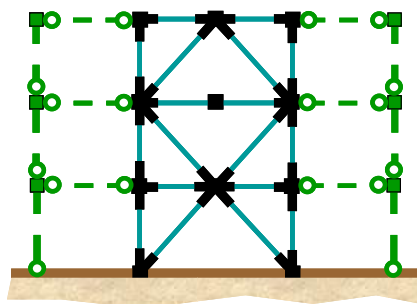


Figure 2.2. Two-dimensional plane frame model with a leaning column

3. ENGINEERING DEMANDS BASED ON NUMERICAL SIMULATIONS

Engineering demand parameters (EDPs) are discussed here in terms of the maximum story drift that occurs during the response to the seismic excitation, the residual (permanent) story drift ratio that presents at the end of the record, and the peak floor acceleration. These EDPs can be related to local structural damage, to damage to displacement sensitive non-structural components and to difficulty in restoring a structure to operational status.

3.1. Story Drift Demands

Fig. 3.1 presents the median and 84th percentile of the maximum story drift of the three SCBF archetypes at three hazard levels, which is the value related to the maximum value of the peak story drift at any story. It is assumed that the distribution of the DR_{max} is lognormal.

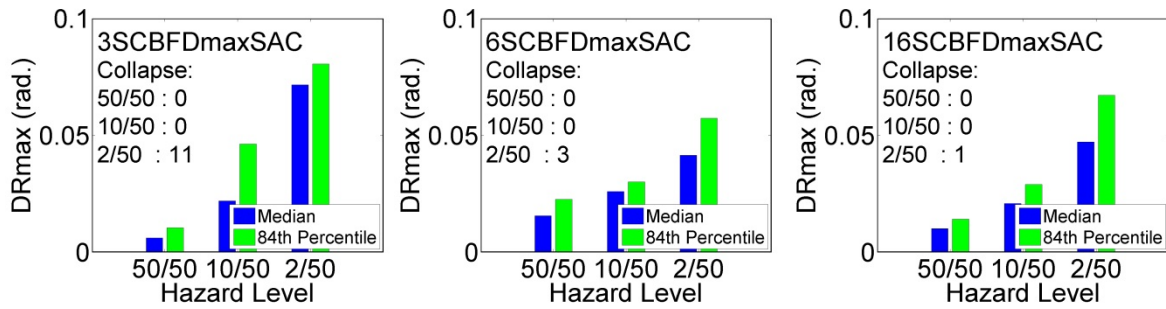


Figure 3.1. Maximum story drift ratios of SCBF archetypes under SAC ground motions corresponding to three hazard levels

The number of cases where the buildings collapsed for these records is also shown in Fig. 3.1; there are 20 records at each hazard level. The results shown are generated from the non-collapse results. If the DRmax of the collapse results were also included, the median and 84th percentile of DRmax would significantly increase, especially for the archetypes with more collapse cases.

At the service-level events, the median DRmax of 3SCBFDmaxSAC is the smallest among the SCBF archetypes compared. At the design-level event, the median DRmax values of the three SCBF archetypes are similar; with values between 2% and 2.6%. The 84th percentile value for 3SCBFDmaxSAC is greater than the other two cases. This large 84th percentile value comes from some near-collapse cases at the design-level event. At the MCE-level event, 3SCBFDmaxSAC shows a total of 11 cases of collapse, which is more collapse cases than the other two archetypes. The median DRmax for the nine excitations where 3SCBFDmaxSAC does not collapse is 7.16%. For 6SCBFDmaxSAC and 16SCBFDmaxSAC, it is 4.14% and 4.71% respectively. In general, for 3SCBFDmaxSAC, the DRmax responses changed more from one hazard level to another than the other two cases. In other words, even if DRmax of 3SCBFDmaxSAC at the service-level event is smaller than other archetypes, DRmax of 3SCBFDmaxSAC at the MCE-level event is larger and contributes to a higher risk of collapse than the other archetypes.

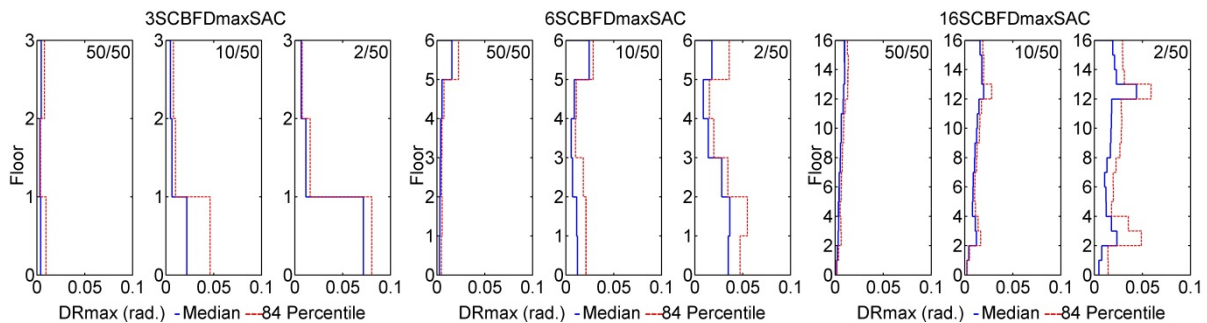


Figure 3.2. Profiles of the maximum story drift ratios of SCBF archetypes under SAC ground motions corresponding to three hazard levels

Fig. 3.2 plots the distribution of the median and 84th percentile of DRmax over the height of the SCBF archetypes. At the service-level event, the DRmaxs were below 0.1% for all SCBF archetypes. The top story of 6SCBFDmaxSAC had the largest median DRmax (1.56%) at the service-level events among the compared models. At the design-level event, 3SCBFDmaxSAC tended to concentrate deformation at the bottom level, while the other archetypes had a more uniform drift profile. For 16SCBFDmaxSAC, the median drifts increased gradually with elevation, but the 84th percentile at the 13th story was large. The drifts at the bottom two stories were small because the available brace sections at these stories were much larger than required and provided extra strength and stiffness. At the MCE-level event, the DRmax profiles were larger than the profile values at the design-level event, but maximum drifts and especially the 84th percentile values tended to be concentrated in a few stories.

3.2. Residual Story Drift Demands

The median residual DRs of SCBF archetypes are less than 0.1% at the service-level event for all three archetypes (see Fig. 3.3). At the design-level event, although the median residual DR of 3SCBFDmaxSAC is 0.52% at the first story, the 84th percentile was more than 2.84%. The median residual DRs of 6SCBFDmaxSAC and 16SCBFDmaxSAC at the design-level event were less than 0.3% and, thus, may be repairable after earthquakes. At the MCE-level event, the residual DRs were especially large at the levels where the median DR_{max} values were concentrated for all three archetypes. The residual DRs of SCBF archetypes with fewer stories tended to be greater than those SCBF archetypes with more stories. Although the median residual DRs of 16SCBFDmaxSAC were the smallest among the three archetypes, i.e. 0.06%, 0.24% and 1.44% for the service-, design-, and MCE-level events, respectively, the 84th percentile value at the MCE-level event was large at the stories where the median DR_{max} was concentrated and exceeded 3.9 making repairs problematic.

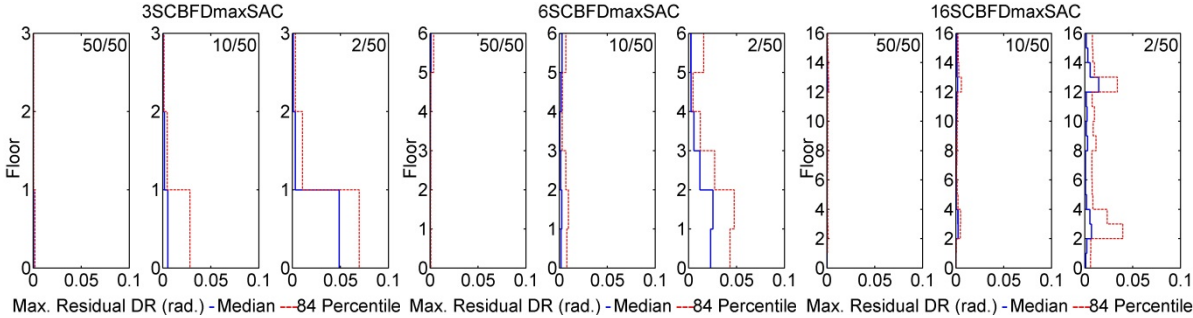


Figure 3.3. Profiles of the maximum residual story drift ratios of SCBF archetypes under SAC ground motions corresponding to three hazard levels

3.3. Floor Acceleration Demand

Life safety hazards can develop as a result of falling objects. The potential for nonstructural elements and contents falling is related to floor level accelerations. In addition to posing a life safety hazard, acceleration sensitive objects can be dislodged or damaged, requiring considerable effort and funds to repair following an earthquake. As such, the maximum peak floor level accelerations are examined.

Fig. 3.4 shows the median and 84th percentile of peak floor acceleration (PFA) of all the archetypes corresponding to various hazard levels; it only accounted for the non-collapse cases. The difference between the 84th percentile and the median shown in Fig. 3.4 illustrates that these differences of SCBF archetypes are between 0.12 g and 0.88 g. The 6-story archetypes had greater difference than 3- and 16-story archetypes, which meant the PFAs had greater variation in the 6-story archetypes. Fig. 3.4 also presents that for all SCBF archetypes, the largest PFAs occur on the bottom and roof floors (or the 5th story of 6SCBFDmaxSAC).

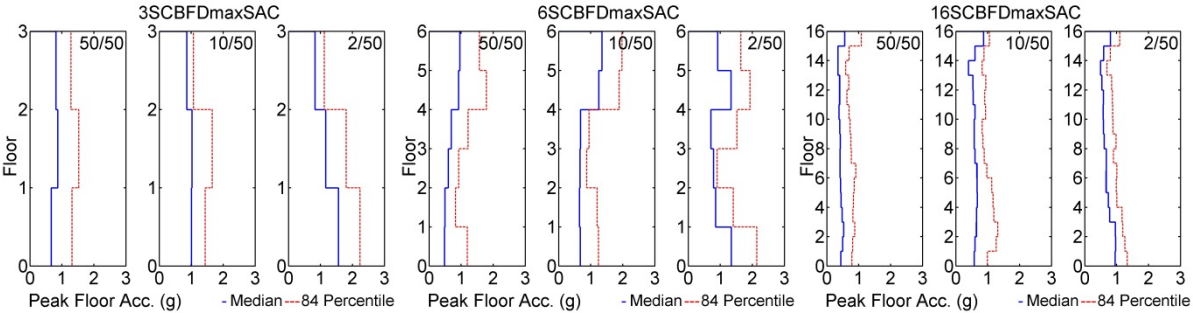


Figure 3.4. Peak floor accelerations of braced frame archetypes with respect to various hazard levels

The median PFAs of low-rise archetypes are generally greater than those of high-rise counterparts.

Note that PFAs at the MCE-level event were generally greater than those at the other hazard levels; this was especially true on the lower floors of all the archetypes. For 16-story SCBF archetype, median PFAs on the higher floors were similar at the design- and MCE-level events and greater than median PFAs at the service-level event.

3.4. Effective R-factors for Design of 2-story SCBF to Resist Collapse

To take advantage of the structural overstrength and ductility, the current code specifies an R-factor. An archetype building, 2SCBFDmaxSAC, which was designed conforming to the current codes, does not have sufficient overstrength and ductility to resist collapse at the MCE-level event. To investigate how to improve the design parameters of low-rise SCBF system, this study discussed the performance of a series of two-story SCBFs designed with various R-factors in the following.

In current code for SCBFs, a design R-factor of 6 resulted in much more than 20% probability of collapse at the MCE-level event for low-rise SCBF archetypes (Chen and Mahin 2010). Table 3.1 summarizes the number of collapses and DR responses of two-story SCBF archetypes with design R-factors of 6, 4.5, 3.3, and 3 under the excitation of SAC ground motions. The archetype with the design R-factor of 6 resulted in one collapse at the design-level event, but the archetype exhibited collapse behavior for almost all the ground motion records at the MCE-level event. In the case where design R-factor of 4.5 was incorporated, the collapse cases were reduced to eight at the MCE-level event, but the collapse risk was still high. When the design R-factor was reduced to 3.3 and 3, no collapse cases were observed at the design-level event and the number of collapse cases at the MCE-level event was only three and one for the archetype of R=3.3 and R=3, respectively.

Table 3.1 also shows the median of maximum DR for these 2-story archetypes. Note that the median DRmax of design R-factor of 6 at the MCE-level event is not shown because only two non-collapse cases remained and the statistical results are not representative. The results demonstrated that considering design R-factors of 3.3 or 3.0 for 2-story SCBF archetypes successfully reduces the drift demand at various hazard levels as well as the probability of collapse at the MCE-level event.

Table 3.1. Summary of responses of 2-story SCBF archetypes with different R-factor for design

R (Design)	T ₁ (Sec.)	Number of Collapses (out of 20 records)		Median DRmax (Non-Collapse)	
		10/50	2/50	10/50	2/50
6	0.4	1	18	0.028	--
4.5	0.35	0	8	0.016	0.033
3.3	0.30	0	3	0.007	0.017
3	0.28	0	1	0.006	0.019

3.5. Out-of-Plane Deformation of Braces

In previous earthquakes, the out-of-plane deformation of braces was commonly seen in SCBF buildings when the gusset plates were oriented to allow braces to move out of the plane. The major concern of out-of-plane deformation of braces is the damage it may cause to the adjacent walls and non-structural components. To prevent such damage, a few design details can easily be employed whereby the braces deform in-plane; such designs are beyond the scope of this research. Although the numerical models presented herein are two-dimensional assuming in-plane buckling of the braces, the investigation of the out-of-plane deformation of braces is possible by measuring the brace deformation transverse to its longitudinal axis. Fig. 3.5 shows the out-of-plane deformation of braces for the SCBF archetypes for three hazard levels. The median out-of-plane deformation at the MCE-level event is 28.7, 22, and 19 inches for 3SCBFDmaxSAC, 6SCBFDmaxSAC, and 16SCBFDmaxSAC, respectively.

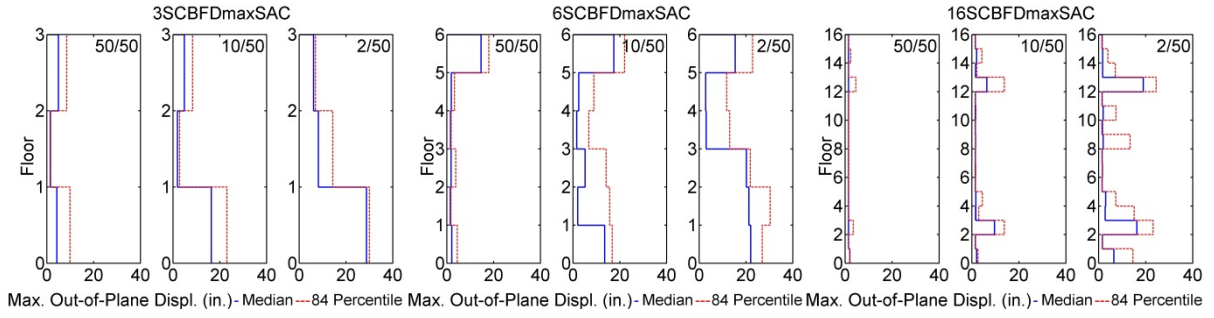


Figure 3.5. Profiles of brace out-of-plane deformation of SCBF archetypes under SAC ground motions corresponding to three hazard levels

The distributions of the out-of-plane deformation along the height of the buildings are similar to the profile of the maximum DR; their relationships were approximately proportional. Fig. 3.6 illustrates the relationship between out-of-plane deformation and the story drift. The story drift caused shortening of the compression braces, which led to out-of-plane deformation of the braces. It was assumed that the axial and flexural deformations of the braces were negligible and the deform shape was composed of straight lines.

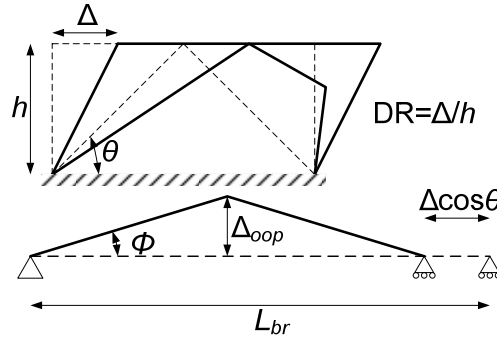


Figure 3.6. Simplified relationship between story drift and brace out-of-plane deformation

The out-of-plane displacement can be expressed as:

$$\begin{aligned}
 \Delta_{oop} &= \frac{L_{br}}{2} \cdot \sin \phi \\
 &= \frac{L_{br}}{2} \cdot \sin \left(\cos^{-1} \left(\frac{L_{br} - h \cdot \cos \theta \cdot DR}{L_{br}} \right) \right) \\
 &= \frac{1}{2} \sqrt{2 \cdot L_{br} \cdot h \cdot \cos \theta \cdot DR - h^2 \cdot \cos^2 \theta \cdot DR^2}
 \end{aligned} \tag{3.1}$$

where $\phi = \cos^{-1} \left(\frac{L_{br} - \Delta \cdot \cos \theta}{L_{br}} \right)$. The brace length is presented by:

$$L_{br} = \eta \cdot \frac{h}{\sin \theta} \tag{3.2}$$

here η is the ratio of hinge-to-hinge length to work point-to-work point length of braces.

In this analysis, the effective brace length was assumed to be 70% of the work point-to-work point length and therefore $\eta = 0.7$. Substituting Eqn. 3.2 into Eqn. 3.1, the out-of-plane displacement can be rewritten and approximated as:

$$\Delta_{oop} = \frac{L_{br}}{2} \sqrt{DR \cdot \frac{\sin 2\theta}{\eta} \left(1 - \frac{\sin 2\theta}{4 \cdot \eta} \cdot DR\right)} \quad (3.3)$$

$$\approx \frac{L_{br}}{2} \sqrt{\frac{\sin 2\theta}{\eta} \cdot DR}$$

The out-of-plane deformation is approximately proportional to square root of DR. Note that when the DR is less than the DR that initiates buckling of the brace, the out-of-plane deformation has not yet occurred and Δ_{oop} should be zero. As such, we modify Eqn. 3.3 as follows:

$$\Delta_{oop} = 0 \quad \text{if } DR \leq DR_{buckle} \quad (3.4)$$

$$\Delta_{oop} \approx \frac{L_{br}}{2} \sqrt{\frac{\sin 2\theta}{\eta} \cdot (DR - DR_{buckle})} \quad \text{if } DR > DR_{buckle} \quad (3.5)$$

where DR_{buckle} is the DR value that initiates buckling of the brace and about 0.25% radian in the analyses.

Tremblay et al. (2003) has derived a simplified relationship between the brace axial deformation and out-of-plane deformation. The relation is re-written in Eqn. 3.6.

$$\Delta_{oop, Tremblay} = 0.7 \sqrt{\Delta \cdot \cos \theta \cdot L_{br}} \quad (3.6)$$

This relation provides a conservative estimate for a low DR demand while giving accurate estimation for large deformations (Tremblay et al., 2003). Fig. 3.7 compares these simplified estimations and the analytical responses of 3SCBFDmaxSAC. Eqn. 3.5 provides accurate estimations of Δ_{oop} for various DR demands especially when the DR demands are small. In other words, Eqn. 3.5 gives more precise information to evaluate damage and loss of SCBF system at various hazard levels for PBEE.

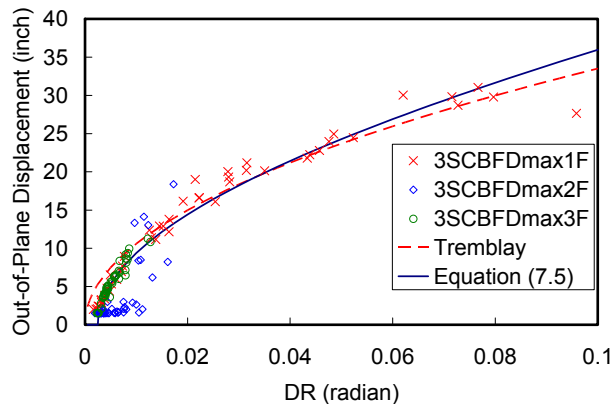


Figure 3.7. Brace Out-of-plane deformation of 3SCBFDmax under SAC ground motions versus predicted relationships

3.6. Ductility Demand of Braces

Local and global buckling of conventional braces results in damage concentration and limits ductility capacity of the braces. To design the braced frame system within the limitation of the ductility capacity of the braces, the ductility demand of braces is investigated. Fig. 3.8 shows a typical hysteresis loop of a conventional buckling brace. The positive and negative ductility is defined and normalized by the yielding deformation of the brace.

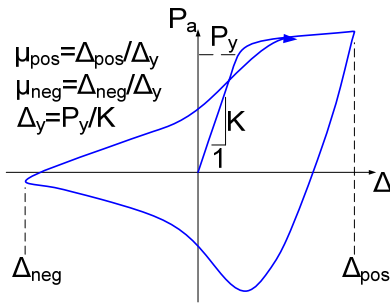


Figure 3.8. Illustration of positive and negative ductility of a conventional buckling brace

Fig. 3.9 shows the ductility demand of SCBF archetypes at various hazard levels. The data only included the non-collapse results.

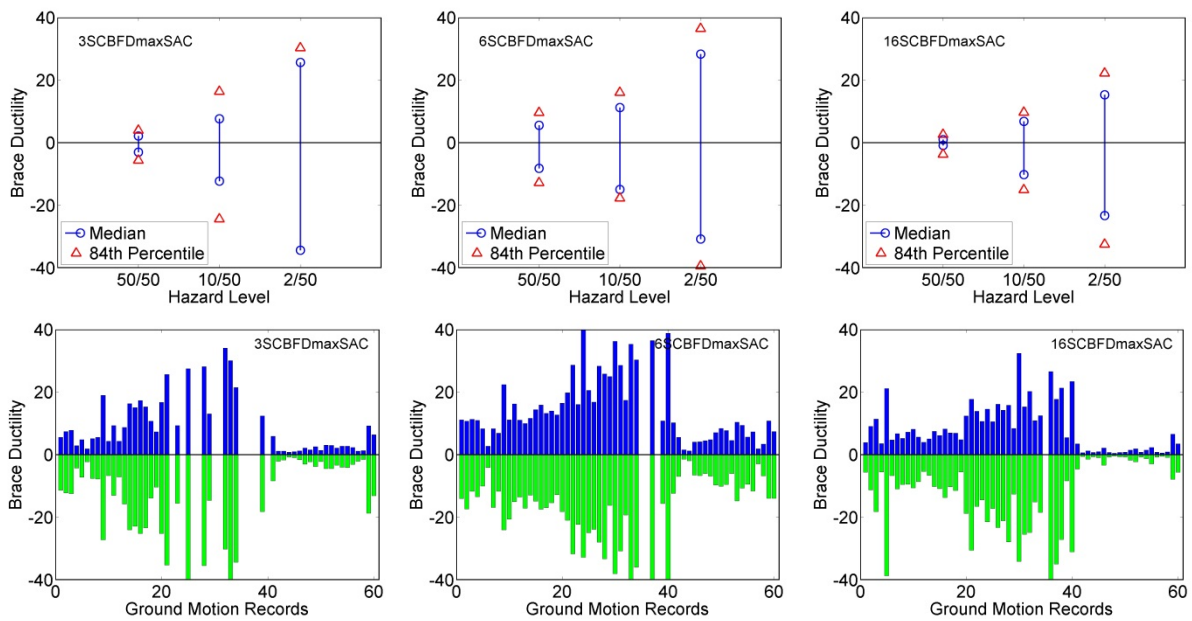


Figure 3.9. Ductility demands of braces in SCBF archetypes under SAC ground motions corresponding to three hazard levels

The distribution of the ductility demand was assumed to be lognormal. For the given SAC ground motions, most of the response of the SCBFs showed a larger ductility demand in the negative direction. At the MCE-level event, the maximum of negative median normalized brace ductility demand, (as exhibited by 3SCBFDmaxSAC), was 34.4. At the design-level event, this occurred in 6SCBFDmaxSAC and is 14.9. The normalized median brace ductility demands of 6SCBFDmaxSAC were greater than those of 3SCBFDmaxSAC at the service- and design-level events, but smaller at the MCE-level event. Archetype 16SCBFDmaxSAC had the smallest brace ductility demands among the SCBF archetypes for the three hazard levels; the normalized median brace ductility demand was 10.2 at the design-level event.

4. CONCLUSIONS

Sixty SAC ground motions representing three hazard levels were applied to investigate the engineering demand parameters of 3-, 6- and 16-story SCBF archetypes. Low-rise SCBF archetypes showed higher probability of collapse at the MCE-level event (Chen and Mahin 2010). The design R-factor of the two-story SCBF archetype was also investigated for its high probability of collapse. The results are summarized below.

The deformation of 3SCBFDmaxSAC archetype tended to concentrate drift in the bottom story. For 16SCBFDmaxSAC, a few of the middle stories had larger median DR_{max} and 84th percentile. Deformation and damage concentration in those stories led to weak stories under dynamic excitations, especially at the MCE-level event.

The median residual DRs at the service- and the design-level events were small (in the order of 0.5% radians) for all archetypes. At the MCE-level event, median residual DRs of all archetypes increase to 1.0% to 3.0%, leading to unreparable damage of the buildings. For 16SCBFDmaxSAC, the maximum median residual DR was 1.44% occurred in only in the 13th story.

The largest median PFAs occurred on the bottom or roof floors (or the 5th story of 6SCBFDmaxSAC) for SCBF archetypes. Analyses showed that the low-rise archetypes had greater median PFAs than the high-rise counterparts, and also showed that PFAs had greater variation in the 6-story archetypes than the other archetypes. In general, median PFAs at the MCE-level event were greater than those at the other hazard levels especially for the lower floor of all SCBF archetypes. Non-structural damage associated with floor acceleration was expected to be more severe for short-period archetypes than for long-period archetypes.

For archetype 2SCBFDmaxSAC, a smaller design R-factor (ex. $R = 3.3$ or $R = 3.0$) is more consistent with the ductility capacity of the structural system and more appropriate for the design. The code mandated R-factor resulted in high probability of collapse at the MCE-level event for short-period SCBF archetypes. The R of 3.3 and 3.0 successfully reduced the drift demand at various hazard levels as well as the probability of collapse at the MCE-level event. It is suggested that a period-dependent design R-factor is more appropriate for the short-period SCBF archetypes in the US.

The out-of-plane deformation is approximately proportional to square root of DR. Note that when the DR is less than the DR that initiates buckling of the brace, the out-of-plane deformation has not occurred yet. The proposed relationship between out-of-plane deformation and DR estimates the out-of-plane deformation accurately at various hazard levels.

The ductility demands of braces show that, in general, the braces deform more in compression than in tension at various hazard levels. In the 16-story SCBF archetype building, the deformation demands of the braces are much less than those in 3- and 6-story SCBF archetype buildings.

REFERENCES

- Chen, C.H., and Mahin, S.A. (2010), "Example Collapse Performance Evaluation of Steel Concentrically Braced Systems," 9th US National and 10th Canadian Conference on Earthquake Engineering: Reaching Beyond Borders, July 25-29, Toronto, Canada.
- FEMA P695 (ATC-63) (2009), *Recommended Methodology for Quantification of Building System Performance and Response Parameters*, Applied Technology Council: Redwood City, CA.
- Khatib, F., Mahin, S. A., and Pister, K. S. (1988), *Seismic behavior of concentrically braced steel frames*, UCB/EERC-88/01, Earthquake Engineering Research Center, University of California, Berkeley, CA.
- McKenna, F. (1997), *Object Oriented Finite Element Programming: Frameworks for Analysis, Algorithms and Parallel Computing*, University of California, Berkeley, Berkeley, CA 94720.
- Somerville, P. G. (1997), *Development of ground motion time histories for phase 2 of the FEMA /SAC Steel Project*, SAC BD/97-04, SAC Steel Joint Venture, Sacramento California.
- Tremblay, R., Archambault, M.-H., and Filiatrault, A (2003), "Seismic Response of Concentrically Braced Steel Frames Made with Rectangular Hollow Bracing Members," *ASCE Journal of Structural Engineering* 129(12), pp. 1626–1636.
- Uriz, P and Mahin, S. (2008), *Towards Earthquake Resistant Design of Concentrically Braced Steel Structures*, PEER-2008/08, Pacific Earthquake Engineering Research Center, University of California, Berkeley, CA.